Journal of Power Sources 248 (2014) 714–720

Contents lists available at ScienceDirect

Journal of Power Sources

journal homepage: www.elsevier.com/locate/jpowsour

Short communication

Estimating the neutrally buoyant energy density of a Rankine-cycle/fuel-cell underwater propulsion system

Daniel F. Waters, Christopher P. Cadou*

Department of Aerospace Engineering, University of Maryland, College Park, MD 20740, USA

HIGHLIGHTS

- Extended earlier work on aluminum–water burning underwater propulsion system.
- Mass estimation methodology extends energy density estimates for neutral buoyancy.
- In neutrally buoyant systems, benefits of fuel cell come with minimal range cost.
- Sensitivity analysis illustrates the influence of design and modeling assumptions.
- Predict up to 5- or 8-fold range improvement over available battery technology.

ARTICLE INFO

Article history:
Received 30 April 2013
Received in revised form
6 September 2013
Accepted 20 September 2013
Available online 7 October 2013

Keywords:
Modeling
Fuel cell
Solid oxide
Aluminum
Underwater
UUV

ABSTRACT

A unique requirement of underwater vehicles' power/energy systems is that they remain neutrally buoyant over the course of a mission. Previous work published in the Journal of Power Sources reported gross as opposed to neutrally-buoyant energy densities of an integrated solid oxide fuel cell/Rankine-cycle based power system based on the exothermic reaction of aluminum with seawater. This paper corrects this shortcoming by presenting a model for estimating system mass and using it to update the key findings of the original paper in the context of the neutral buoyancy requirement. It also presents an expanded sensitivity analysis to illustrate the influence of various design and modeling assumptions. While energy density is very sensitive to turbine efficiency (sensitivity coefficient in excess of 0.60), it is relatively insensitive to all other major design parameters (sensitivity coefficients < 0.15) like compressor efficiency, inlet water temperature, scaling methodology, etc. The neutral buoyancy requirement introduces a significant ($\sim$15%) energy density penalty but overall the system still appears to offer factors of five to eight improvements in energy density (i.e., vehicle range/endurance) over present battery-based technologies.

1. Introduction

The United States Navy has identified certain key naval missions like intelligence, surveillance, and reconnaissance as being best performed by Unmanned Undersea Vehicles (UUVs) [1]. Critical to the success of these missions are compact, quiet, and highly efficient power and energy systems that enable long range and endurance [1]. Previous work [2–4] explored the viability of an unusual propulsion system called the Hybrid Aluminum Combustor (HAC) based on the exothermic reaction of aluminum with seawater. It used a comprehensive thermodynamic analysis to predict the overall efficiency and volume of this system. These data were used to compute the system's effective volumetric energy density so that it could be compared to that of other power and energy systems. However, this analysis was done without regard to the system's overall density. This is important as most underwater vehicles must be neutrally buoyant [5] and making them so usually requires adding empty volume which lowers overall energy density – often significantly. Therefore, the objective of this 'short communication' is to correct previous estimates of the aluminum–water propulsion system's performance for the effects of the neutral buoyancy requirement so that power and energy systems can be compared on a more appropriate baseline. This will be accomplished by updating earlier models of a 1000 L aluminum combustion-based power section (appropriate for use in heavy-weight to large class UUVs [1,6]) to predict the mass of individual components (in addition to their volume) and by introducing appropriate 'dead' volume to ensure that the overall system is neutrally buoyant. This empty volume can

* Corresponding author. Tel.: +1 301 405 0829; fax: +1 301 314 9001.
E-mail address: cadou@umd.edu (C.P. Cadou).

0378-7753/$ – see front matter © 2013 Elsevier B.V. All rights reserved.
http://dx.doi.org/10.1016/j.jpowsour.2013.09.113

Nomenclature

A_{cross}	cross sectional area
BOP	balance of plant
C_D	drag coefficient
C_P	specific heat capacity
CEA	chemical equilibrium with applications
ED_V	volumetric energy density
HAC	hybrid aluminum combustor
L	length
M	mass
$\dot{m}$	mass flow rate
MEA	membrane electrode assembly
N	number/quantity
n	mass scaling exponent
NPSS	numerical propulsion system simulation
S_X	sensitivity coefficient with respect to parameter X
SOFC	solid oxide fuel cell
UUV	unmanned undersea vehicles
V	volume
v_C	cruise velocity
$\dot{W}$	power
ΔH_V	volumetric energy content
Δt	elapsed time, endurance
ε	heat exchanger effectiveness
η_p	propulsive efficiency
η_t	thermodynamic efficiency
ρ	density

Subscripts

C	cold side property
cell	single fuel cell property
comp	component
H	hot side property
HE	heat exchanger
inlet	property at component inlet
parts	internal parts of machinery
PL	payload
reac	reactant
reacted	amount consumed by reaction
ref	reference state
stack	fuel cell stack
sys	system property

also be used to keep system mass constant and maintain neutral buoyancy by storing waste products or water to balance the consumed reactants. The effects of hydrogen utilization (i.e., the percentage of H_2 generated by the Al–H_2O reaction that is consumed by the fuel cell) and operating depth are also re-explored in the context of the neutral buoyancy requirement.

2. Propulsion system concept

Fig. 1 is a schematic illustration of the HAC system with integrated solid oxide fuel cell (SOFC) investigated in Ref. [4]. The SOFC produces power in a way that increases overall system efficiency while enabling periods of all electric operation. It also converts the large volumes of waste H_2 produced by the aluminum–seawater reaction to liquid water that is much more easily stored.[1] The system operation is described in detail elsewhere [2,4,7] and is only briefly summarized here: a fuel feeder produces a stream of aluminum powder suspended in H_2 gas which reacts with steam to form Al_2O_3, more H_2, steam, and heat. The flow passes through a separator to remove the aluminum oxide. A portion (20–25%) of the flow is recirculated to sustain the reaction in the combustor. The remainder passes through a turbine that extracts mechanical power. The flow passes to the SOFC where a fraction of the hydrogen (the 'H_2 utilization') is consumed to produce electric power. A heat exchanger then transfers waste enthalpy in the exhaust to prewarm the incoming water. The remaining steam is fully condensed and supplemented with seawater to make up for what was consumed by the reaction. A portion of the H_2 gas is separated from the condensed water, compressed, and reused for the aluminum feeder. Any *remaining* H_2 must be vented overboard unless a fuel cell is also present. Incorporating a fuel cell requires the following additional components: an oxidizer tank (63% by mass H_2O_2), a membrane electrode assembly (MEA), a condenser and separator to trap and remove the water produced in the MEA, and a compressor to return unused O_2 to the cathode. A decomposition reactor is also added to facilitate the breakdown of H_2O_2 to H_2O and O_2 although it could be possible to do this directly on the SOFC's cathode.

[1] Stealth considerations often prohibit dumping the Al_2O_3 and H_2 waste produced by the Al–H_2O overboard. However, the thermodynamic cost of compressing and storing H_2 on board can be large [7]. The ready availability of cooling water makes it much simpler to achieve isothermal compression – heat exchangers can be smaller, integrated into the hull, etc. – but there is a complex tradeoff between the efficiency gain and the volume displaced by these additional components. Exploring this tradeoff is beyond the scope of this work and attention focuses instead on identifying the limits of system performance associated with adiabatic vs. isothermal compression.

3. Model formulation

3.1. Simulation environment

Mathematical models are developed for each component and are coupled and solved in an environment called Numerical Propulsion System Simulation (NPSS) [8]. Models can range from simple algebraic equations to links to external thermodynamic solvers like chemical equilibrium analysis (CEA) [9] or computational fluid dynamics packages. Additional information about NPSS and the individual component models is available elsewhere [4,8].

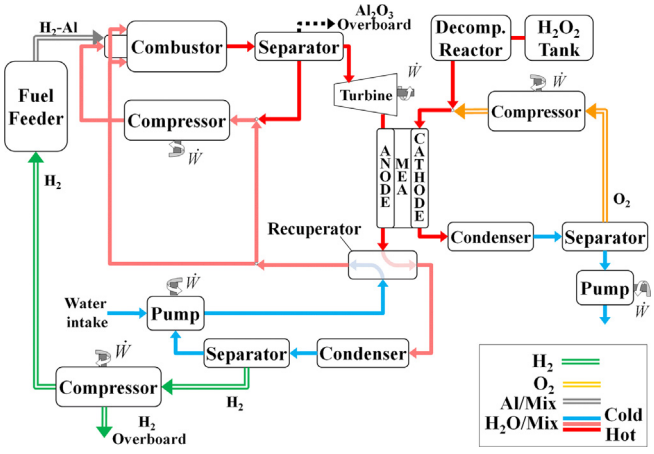

Fig. 1. Diagram of the HAC-SOFC hybrid system from Ref. [4].

The focus here will be on the modifications made to the earlier model [4] to enforce neutral buoyancy.

3.2. Equations for UUV range and endurance

The range and endurance of a UUV cruising at constant speed (v_C) are given by [7]:

$$\text{Range} = \frac{\eta_p \cdot ED_V \cdot V_{sys}}{\left(\dot{W}_{PL}/v_C\right) + \left(\frac{1}{2}\rho_{seawater} v_C^2\right) \cdot (C_D A_{cross})} \quad (1)$$

$$\text{Endurance} = \Delta t = \frac{\eta_p \cdot ED_V \cdot V_{sys}}{\dot{W}_{PL} + \left(\frac{1}{2}\rho_{seawater} v_C^3\right) \cdot (C_D A_{cross})} \quad (2)$$

In these expressions, C_D is the vehicle drag coefficient, $\dot{W}_{PL}$ is the payload power, A_{cross} is the vehicle cross-section area, V_{sys} is the total volume of the power and energy system, η_p is the propulsive efficiency, and ED_V is the 'effective' energy density of the power and energy system. The 'effective' energy density is the total recoverable energy available in the system divided by the total system volume:

$$ED_V = \eta_t \cdot \Delta H_{V,reac} \cdot \frac{V_{reac}}{V_{sys}} \quad (3)$$

In this expression, $\Delta H_{V,reac}$ is the volumetric energy density of reactants, V_{reac}/V_{sys} is the fraction of total system volume allocated for reactant storage, and η_t is the thermodynamic efficiency of the power and energy system. Since the objective is to evaluate the aluminum combustor/SOFC system as a 'drop in' replacement for existing power and energy systems, V_{sys} and η_p are assumed to be fixed here and ED_V is the performance parameter of interest.

3.3. Volume and mass scaling

The volume of each component is assumed to be directly proportional to the flow passing through it so that components get larger or smaller with the design power requirement of the system. Each component is assumed to be cylindrical, flow velocities through them are assumed to be uniform, and residence time is assumed to be constant. These assumptions lead to Eq. (4) which describes how the volume of a component varies with respect to a reference size associated with the baseline system. Reference states for various components consistent with a 15 kW system are listed in Table 1.

$$V_{comp} = V_{comp,ref}\left(\frac{\dot{m}}{\dot{m}_{ref}}\right) \quad (4)$$

Heat exchangers are assumed to be simple straight tube, countercurrent designs. An iterative finite differencing scheme is applied [7] to determine the appropriate length (L). The volume of the heat exchanger also depends on the required effectiveness (ε) and heat capacity ratio between the streams ($\dot{m}_H C_{P,H}/\dot{m}_C C_{P,C}$).

$$V_{HE} = V_{HE,ref}\left(\frac{\dot{m}}{\dot{m}_{ref}}\right) \cdot \frac{L\left[\varepsilon, \left(\dot{m}_H C_{P,H}/\dot{m}_C C_{P,C}\right)\right]}{L\left[\varepsilon_{ref}, \left(\dot{m}_H C_{P,H}/\dot{m}_C C_{P,C}\right)_{ref}\right]} \quad (5)$$

The volume of the fuel cell is estimated based on the required number of cells (determined by dividing the total required electric power by the design power output of a single cell), prior estimates of the mass and volume of an individual cell (0.033 kg and 0.033 L for a 64 cm^2 cell [10]), and the assumption that the SOFC system volume (V_{SOFC}) including pipes and pumps is 3 times the volume of the stack alone (V_{Stack}) [10]. Although this approach neglects additional factors that could arise in the case of a very large stack (which could require proportionally more structural support and less insulation), it provides a reasonable approximation.

$$V_{SOFC} = \left(\frac{V_{SOFC}}{V_{Stack}}\right) \cdot N_{cell} \cdot V_{cell} = \left(\frac{V_{SOFC}}{V_{Stack}}\right) \cdot \left(\frac{\dot{W}_{SOFC}}{\dot{W}_{cell}}\right) \cdot V_{cell} \quad (6)$$

The mass of a component is assumed to scale with its volume according to Eq. (7) where the parameter n represents the nature of the scaling. A value of $n = 1$ corresponds to a linear scaling of component mass with volume. This is valid for thin walled cylindrical pressure vessels where, for a fixed operating pressure, wall thickness is proportional to the radius [11] and therefore wall mass is proportional to radius squared times length (i.e., volume). A value of $n = 2/3$ corresponds to a situation where mass scales roughly with surface area. This is valid for a vessel with constant wall thickness. The influence of the choice of scaling exponent will be examined by comparing results obtained using each assumption.

$$\frac{M_{comp}}{M_{comp,ref}} = \left(\frac{V_{comp}}{V_{comp,ref}}\right)^n \quad (7)$$

The mass of the reference configuration (Table 1) was estimated using the following very basic sizing techniques. The component wall thicknesses were selected to withstand pressure stresses using standard techniques for cylindrical pressure vessel design [11] and a factor of safety of 2. The remaining mass is determined by making some basic assumptions about the internal design of turbines, compressors, heat exchangers, etc. in order to estimate a 'packing factor' equal to the fraction of interior volume filled by structural elements or mechanical parts ($=V_{parts}/V_{comp}$). A 'packing factor' of 1 corresponds to solid block whereas 0 corresponds to a hollow shell. The 'packing factors' used in this work are listed in Table 1. The largest factors are for the pumps, turbine, and compressors which have lots of moving parts. The smallest factor is for the combustor which is a nearly hollow chamber. Most components are assumed to be constructed from aluminum but titanium alloys are assumed for high temperature components like the combustor and turbine.

Table 1
HAC system component reference states.

Component	$\dot{m}_{ref}$ (kg s^{-1})	$V_{comp,ref}$ (L)	'Pack factor'	$M_{comp,ref}$ (kg)
Fuel feeder	0.0147	6.25	0.25	5.0
Combustor	0.0835	50	0.05	14.2
Oxide separator	0.0835	25	0.15	18.1
Steam compressor	0.0147	6.25	0.35	10.1
Steam turbine	0.0571	25	0.35	40.3
Heat exchanger	0.1159	62.5	0.30	63.2
Water pumps	0.0587	25	0.35	23.8
Condenser	0.0571	20	0.20	10.8
H_2 separator	0.0571	25	0.15	10.2
H_2 compressors	0.0014	5	0.35	4.8

3.4. Energy density calculations

The system volume is the sum of the HAC, SOFC, reactants, and any empty volume needed to achieve neutral buoyancy. The mass available for reactant (fuel) storage is found by requiring that the total mass of the system equals the volume of the system times the density of water. This leads directly to an expression for the volume

[2] Note that the 47% number depends on the performance of the aluminum seeder and could be different for different systems.

of fuel required, Eq. (8). Rewriting the product of efficiency and reaction enthalpy from Eq. (3) as the ratio of system power to reactant flow rate gives Eq. (9) for the system energy density in terms of the quantities in the model.

$$V_{reac} = \frac{\rho_{water} V_{sys} - M_{HAC} - M_{SOFC}}{\rho_{reac}} \quad (8)$$

$$ED_V = \left(\dot{W}_{HAC} + \dot{W}_{SOFC}\right) \frac{\rho_{reac}}{\dot{m}_{reac}} \frac{V_{reac}}{V_{sys}} \quad (9)$$

4. Results and discussion

4.1. Operating cases considered

The H_2 utilization rate ($= \dot{m}_{H_2,reacted}/\dot{m}_{H_2,inlet}$) is set to 0% for the first model run in order to establish a baseline corresponding to a HAC system operating without a fuel cell. The full range of available H_2 utilizations is examined from 0% up to 53% where all of the 'excess' H_2 is consumed. The remaining 47% of the H_2 produced by the Al–H_2O reaction is needed to operate the aluminum feeder.[2] In this analysis, any 'excess' H_2 is assumed to be vented overboard and the work required to compress it to the ambient pressure (so that it can be dumped) is accounted for when computing the net power output of the system. Depths of 3 m (131.7 kPa), 30 m (407.5 kPa), and 150 m (1633.4 kPa) are investigated to cover the operating range defined as necessary by the Navy for UUVs in this class [6,12].

Calculations for each case begin at 0% H_2 utilization and 15 kW net power output. This power level is chosen in order to be consistent with a 1000 L power section operating at 10–20 W L^{-1} power density [12]. The HAC system is scaled as required by varying the fuel mass flow (which in turn causes other flows in the system to vary). The efficiencies of all components are assumed to remain constant over the duration of the mission.

4.2. Effects of H_2 utilization and depth

Fig. 2 shows energy density as a function of fuel cell H_2 utilization assuming adiabatic (lower) and isothermal (upper curves) H_2 compression at 70% adiabatic and isothermal efficiency, respectively. Recall that adiabatic and isothermal compressions are assumed to identify the lower and upper bounds of system performance respectively. The thick curves correspond to the assumption that HAC mass scales linearly with volume, and the thin curves just below them correspond to the assumption that mass is proportional to surface area. The linear scaling leads to higher energy densities than predicted by area proportional scaling. However, the difference is relatively small (1%–3.5%) so the linear scaling is used for the rest of the calculations reported here.

With adiabatic compression at 3 m, the system delivers a neutrally buoyant energy density of 277 W h L^{-1} at 0% H_2 utilization (i.e., the baseline HAC system) and 509 W h L^{-1} at full (53%) utilization. The neutrally buoyant energy density peaks at 532 W h L^{-1} and 35% H_2 utilization because of a competition between system efficiency (which is improved by incorporating the fuel cell) and the displacement of fuel by the fuel cell system. With isothermal compression at 3 m, the system delivers a neutrally buoyant energy density of 714 W h L^{-1} (the maximum observed) at 0% H_2 utilization and 606 W h L^{-1} (15% below peak) at full utilization. No peak is observed because of the improved H_2 compression efficiency. Switching to isothermal compression more than doubles the energy density of the system at zero H_2 utilization. Isothermal compression improves energy density by 19% at full utilization. While these results suggest that increasing system complexity by using cooled compressors could be very worthwhile, this only represents an upper bound on what is possible thermodynamically because no accounting has been made for the additional volume required and the performance of a real 70% efficient system would be less. The effects of increasing vehicle depth are also clear in Fig. 2: As depth is increased, more work is required to raise the hydrogen to the ambient pressure which reduces system energy density. The curves converge at full H_2 utilization where there is no need to vent excess H_2 and the system becomes depth independent. However, if stealth is required (i.e., venting H_2 overboard is prohibited) then the best performance always occurs at 100% H_2 utilization.

Fig. 3 compares the neutrally buoyant results to those previously reported [4] for negatively buoyant (denser than water) systems. Only results at 3 m depth are shown (recall that surface area proportional mass scaling results will be 1–3.5% lower). The comparison shows that the penalty associated with enforcing neutral buoyancy is quite large: energy density is reduced by 58% at zero H_2

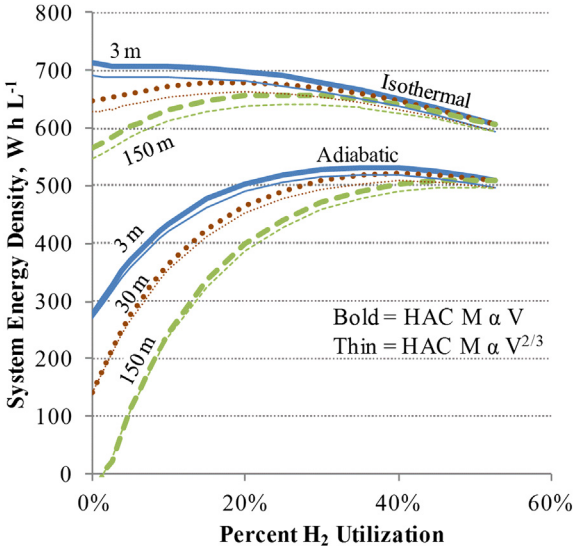

Fig. 2. System energy density vs. hydrogen utilization under neutrally buoyant conditions at various depths.

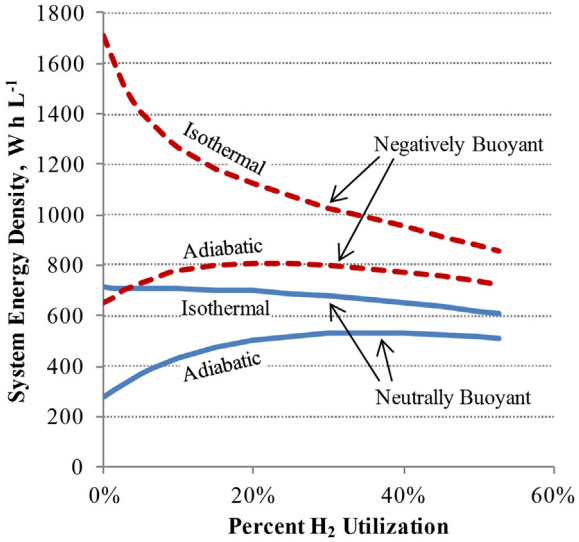

Fig. 3. System energy density vs. hydrogen utilization, comparison of neutral and negative buoyancy.

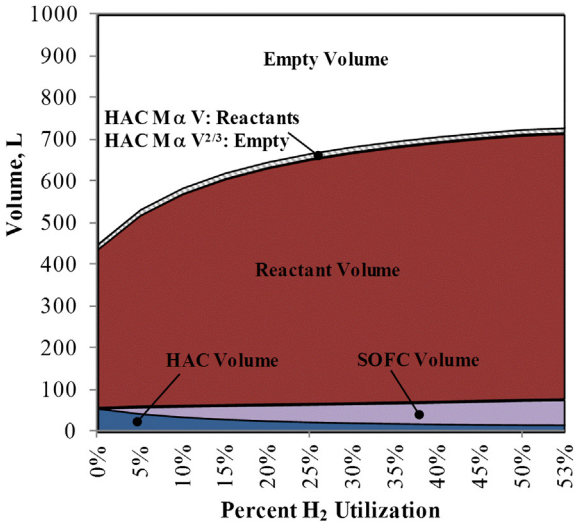

Fig. 4. Component volume vs. hydrogen utilization for neutrally buoyant system at 3 m depth. Isothermal compression is assumed.

utilization and by 29% at full utilization for either the adiabatic or isothermal compression cases. The penalty is smaller at high utilization because the fuel cell and H_2O_2 are less dense than the HAC and aluminum they displace. This is illustrated in Fig. 4 which shows the volume distribution in the 1000 L power and energy section as a function of H_2 utilization for the neutrally buoyant system at 3 m depth using isothermal compression. The HAC, SOFC, and reactant storage volumes are shown along with the empty volume necessary to achieve neutral buoyancy. The small cross-hatched volume illustrates the difference between the predictions of the two mass scaling assumptions. Assuming HAC mass proportional to volume predicts a slightly lighter system which allows for more reactant storage and thus higher overall system energy density. The figure shows that the volume that must be left empty at zero utilization is approximately twice that required at full utilization and so the penalty associated with adding the fuel cell is reduced. The net result is that for isothermal compression at a depth of 3 m, adding the fuel cell only drops the neutrally buoyant energy density by 15% compared to 50% in the denser than water system. Therefore, the benefits of adding a fuel cell (eliminating H_2 venting, depth independence, enabling periods of all electric operation) come at much smaller cost when the effects of maintaining neutral buoyancy are factored in.

4.3. Sensitivity analysis

Since so many assumptions must be made in analyses of this type, it is useful to quantify the impact of the impact of these assumptions on the predicted energy density. This is accomplished by computing 'sensitivity coefficients' (S_X) for each parameter X. It is defined as the fractional change in system energy density divided by the fractional change in the parameter as shown in Eq. (10) where '*ref*' refers to the baseline assumptions and results and prime values denote the values of the perturbed parameter and the resulting energy density.

$$S_X = \frac{\left(ED'_v - ED_{V,ref}\right)/ED_{V,ref}}{\left(X' - X_{ref}\right)/X_{ref}} \tag{10}$$

The results of the sensitivity analysis are shown in Fig. 5. All changes are relative to the neutrally buoyant HAC system (HAC mass αV) with an isothermal compression system operating at 3 m depth and full utilization. The various parameters investigated are grouped into four categories: component performance parameters (turbine efficiency, compressor efficiencies, fuel seed ratio), fuel cell material properties (electrode porosity and tortuosity, thickness of electrodes and electrolytes), system operating parameters (temperatures, pressures, current density, power demand), and scaling assumptions (reference masses and volumes).

The figure shows that the turbine efficiency has by far the largest impact on the overall system energy density and thus is the most important parameter to know well. The value used here (0.60) is well below typical values for large, state of the art steam turbines. The value is chosen to be a conservative estimate for smaller sized machines in this type of application [13]. Another particularly important parameter is the H_2 compressor efficiency. The value used here (0.70) is a conservative estimate for typical hydrogen compressors [14].

Several system operating parameters also have important influences on cycle performance, but unfortunately the operator has only limited ability to control many of them. The incoming water temperature is set by environmental conditions, turbine pressure ratio is limited by system pressures, and power demand is set by mission requirements. Note that the assumed inlet water temperature (21 °C) is relatively high (allowing for seasonal and regional differences), and operating at temperatures that are more representative of ocean averages would substantially improve performance. The results also show that it would be beneficial to raise overall system pressures, but this will be limited by the need to

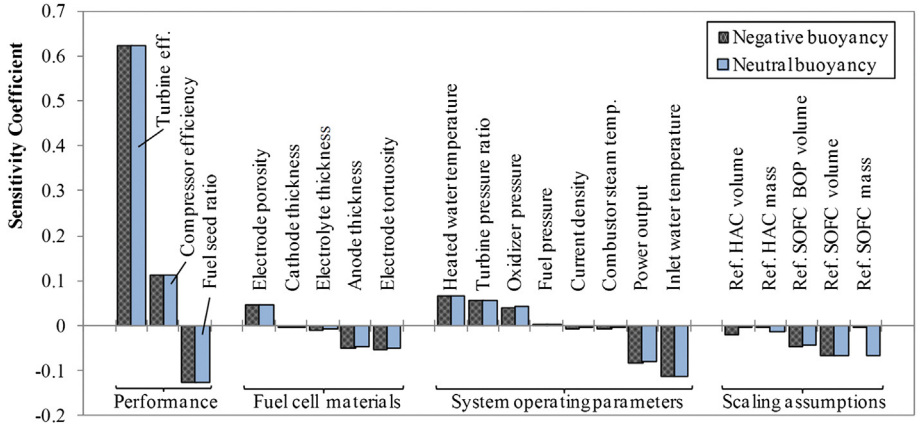

Fig. 5. Sensitivity of overall system energy density to different system properties and design assumptions.

increase wall thicknesses, etc. to withstand higher pressures. The additional mass that this would require is not accounted for in the current model. The properties of the materials used to construct the fuel cell also have significant impacts on energy density, but their importance is at least an order of magnitude smaller than the turbine efficiency. For example, the electrodes' porosity and tortuosity control diffusion and thus the diffusion overpotential. Anode thickness has more impact than cathode or electrolyte thickness because of the importance of anode diffusion in this particular SOFC arrangement. The values of these parameters are consistent with those used in other SOFC modeling studies [15–18]. Sensitivities to choices of SOFC reference mass, volume, and balance of plant (BOP) volume are also approximately one order of magnitude smaller than the sensitivity to turbine efficiency. The volume of the SOFC balance of plant components is related to the V_{SOFC}/V_{stack} parameter [10] discussed in Section 3.3 (i.e., $V_{BOP}/V_{stack} = V_{SOFC}/V_{stack} - 1$). The choice of SOFC reference mass and volumes have larger impacts than the choice of HAC reference volume and mass because at full utilization the SOFC is the larger system.

Boundaries on the overall (cumulative) uncertainty in the predicted energy density were estimated by perturbing all of the design parameters by 10% in a coordinated manner so that they either raise or lower the overall system energy density. The results show that a ±10% shift in these parameters translates to a ±15% shift in predicted energy density. Since it is unlikely that the values of all of the design parameters would be off by 10% and that the deviations would all bias the energy density in the same direction, 15% most likely represents an upper bound on the uncertainty of the energy density estimates.

4.4. Overall performance comparison

Fig. 6 compares predicted energy densities for HAC and HAC-SOFC systems to those of other UUV power systems based on SOFCs [10], lithium-ion [19–21], lead-acid [21], and silver-zinc [21] battery systems. Results for both the present (neutrally buoyant, both scaling assumptions) and past (negatively buoyant [4]) studies are presented for comparison. The 'error' bars indicate the approximate range of performance that one could expect based on the reports in the literature. For the HAC systems, the solid portion of the bars shows the performance with adiabatic compression. The very top of the cross-hatched bars shows the performance that is possible with an isothermal compressor that adds negligible mass and volume compared to an adiabatic compressor. The intermediate lines in the cross-hatched portion show the peak performance for isothermal compression systems of various masses and volumes.

The figure shows that six- or seven-fold improvements in neutrally buoyant system energy density are possible over existing Li-ion battery technology with compact isothermal compression. While the neutral buoyancy requirement results in a significant drop in energy density, battery-based systems suffer similar penalties. The pure SOFC system fares better under the neutrally buoyant restriction because the system defined in Ref. [10] is already nearly neutrally buoyant. Note that it only slightly underperforms the peak performance of the HAC and HAC-SOFC systems.

The neutral buoyancy constraint also greatly reduces performance differences between the various HAC cases compared to the earlier results in the heavier than water systems. This is an important finding because the earlier results suggested that eliminating gas venting and achieving depth insensitivity came at very large cost in terms of reduced performance. The present results show that in neutrally buoyant systems, much less performance must be sacrificed in order to achieve the important benefits offered by the HAC-SOFC hybrid system.

5. Conclusions

An earlier numerical model of an underwater power system has been expanded to account for the fact that most underwater power and energy systems must be neutrally buoyant. While this imposes a substantial energy density penalty, other systems suffer similar penalties and the hybrid aluminum combustor/solid oxide fuel system fares proportionally better. Another key finding is that the neutrally buoyant systems show far less variation between the straight aluminum burning system and the fuel cell hybrid system. This means that the benefits of the fuel cell (elimination of H_2 venting, depth independence, and enabling periods of all electric operation) are achieved with minimal performance penalty. Finally, a sensitivity analysis shows that the performance of the turbine has by far the largest impact on the overall energy density achievable by the system. The baseline model assumptions suggest that energy

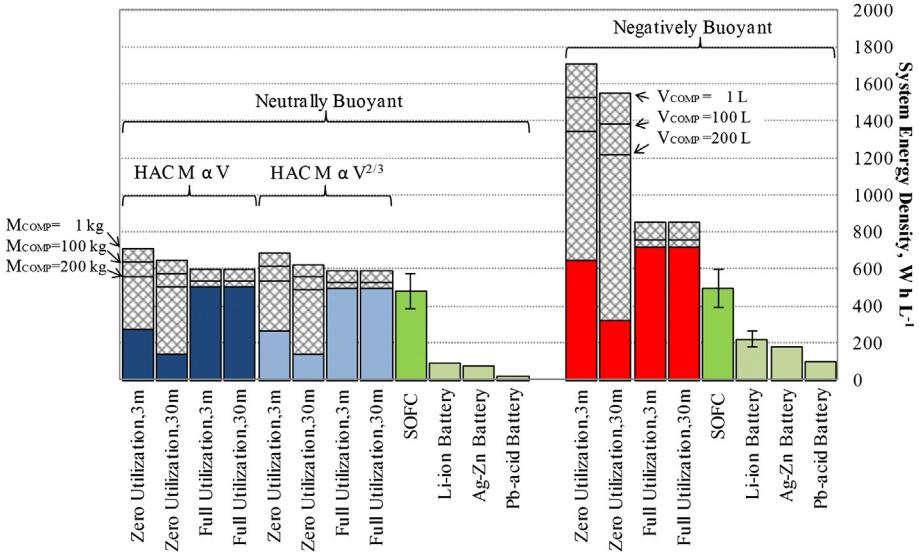

Fig. 6. Comparison of the energy densities of various underwater power and energy technologies.

density improvements of factors of 6–7 over current technology (batteries) are possible. This range broadens to factors of 5–8 improvements in overall system energy density when uncertainties in the model's assumptions and the system's sensitivity to them are accounted for. Therefore, the aluminum combustion system appears to be an extremely promising power/energy source for unmanned underwater vehicles.

Acknowledgments

The authors would like to thank Dr. Joseph Fontaine of the Naval Undersea Warfare Center–Newport Branch, Mr. Tom Lavelle of the NASA Glenn Research Center, and Dr. Greg Jackson of the Colorado School of Mines for their help and guidance, and Ms. Maria Medeiros and the Office of Naval Research for their support of the original study under contract N00014-08-1-0717.

References

[1] The Navy Unmanned Undersea Vehicle (UUV) Master Plan, Department of the Navy, 2004.
[2] W.E. Eagle, M.S. Thesis, University of Maryland – College Park, 2007.
[3] D.F. Waters, C.P. Cadou, W.E. Eagle, J. Propul. Power 29 (3) (2013) 675–685.
[4] D.F. Waters, C.P. Cadou, J. Power Sources 221 (2013) 272–283.
[5] A.A. Burke, L.G. Carreiro, E.S. Greene, J. Power Sources 176 (2008) 299–305.
[6] Large Displacement Unmanned Underwater Vehicle Innovative Naval Prototype Energy Section Technology, Office of Naval Research, 2011. BAA #11-028.
[7] D.F. Waters, M.S. Thesis, University of Maryland – College Park, 2011.
[8] NPSS User Guide, Software Release 1.6.5, NASA, 2008.
[9] B. McBride, S. Gordon, Computer Program for Calculation of Complex Chemical Equilibrium Compositions and Applications II, in: User's Manual and Program Description, NASA Publication, 1996. RP-1311–P2.
[10] A.A. Burke, L.G. Carreiro, J. Power Sources 158 (2006) 428–435.
[11] J.P. Den Hartog, Strength of Materials, Dover Publications, Mineola, NY, 1977, pp. 136–146.
[12] Long Endurance Undersea Vehicle Propulsion, Office of Naval Research, 2011. BAA #11-016.
[13] T.F. Miller, J.L. Walter, D.H. Kiely, Workshop on Underwater Vehicles, June 20–21, 2002.
[14] E. Tzimas, C. Filiou, S.D. Peteves, J.B. Veyret, Hydrogen Storage: State-of-the-art and Future Perspective, European Commission, Directorate General Joint Research Centre, Institute for Energy, Petten, The Netherlands, 2003.
[15] R.J. Kee, H. Zhu, A.M. Sukeshini, G.S. Jackson, Combust. Sci. Technol. 180 (2008) 1207–1244.
[16] H. Zhu, R.J. Kee, J. Power Sources 169 (2007) 315–326.
[17] H. Zhu, R.J. Kee, V.M. Janardhanan, O. Deutschmann, D.G. Goodwin, J. Electrochem. Soc. 152 (2005) A2427–A2440.
[18] H. Zhu, R.J. Kee, J. Power Sources 117 (2003) 61–74.
[19] J.B. Lakeman, A. Rose, K.D. Pointon, D.J. Browning, K.V. Lovell, S.C. Waring, J.A. Horsfall, J. Power Sources 162 (2006) 765–772.
[20] R. Gitzendanner, F. Puglia, C. Martin, D. Carmen, E. Jones, S. Eaves, J. Power Sources 136 (2004) 416–418.
[21] M. Adams, W. Halliop. Biloxi, MS, MTS/IEEE Oceans '02, vol. 1, October 19–31, 2002, pp. 199–202.